



# The investigation of thermal pyrolysis of glycerol carbonate derivatives by TG–FTIR



Rujuan Li<sup>a</sup>, Jing Liu<sup>a,\*</sup>, Hairong Tao<sup>b</sup>, Donglan Sun<sup>c</sup>, Dagang Xiao<sup>a</sup>, Chunjing Liu<sup>a</sup>

<sup>a</sup> College of Chemical Engineering and Material Science, Tianjin University of Science & Technology, Tianjin 300457, China

<sup>b</sup> College of Chemistry, Beijing Normal University, Beijing 100875, China

<sup>c</sup> College of Science, Tianjin University of Science & Technology, Tianjin 300457, China

## ARTICLE INFO

### Article history:

Received 21 September 2015

Received in revised form 6 December 2015

Accepted 9 December 2015

Available online 14 December 2015

### Keywords:

GC derivatives

Thermal stability

Thermal pyrolysis

TG–FTIR

Bond dissociation energy

## ABSTRACT

Three new GC derivatives, carbonic acid bis-(2-oxo-[1,3]dioxolan-4-ylmethyl) ester (CABE), succinic acid bis-(2-oxo-[1,3]dioxolan-4-ylmethyl) ester (SABE) and terephthalic acid bis-(2-oxo-[1,3]dioxolan-4-ylmethyl) ester (TABE), were designed and synthesized. We investigated the thermal stability and the thermal pyrolysis of three compounds by TG–FTIR, and the bond dissociation energy was calculated to further demonstrate the decomposition process. The results showed that the three GC derivatives had one, two, three weight loss stages, respectively. Their initial decomposition temperature was as high as 200 °C, which means that the compounds have good thermal stability. 5% weight loss temperature was increased in the order of TABE > SABE > CABE. In thermal pyrolysis process, the C–C, C–O bonds of cyclic carbonate fractured preferentially, and then the C–O bonds nearby cyclic carbonate of SABE and TABE continued to fracture to produce linear ester in the form of fragment.

© 2015 Elsevier B.V. All rights reserved.

## 1. Introduction

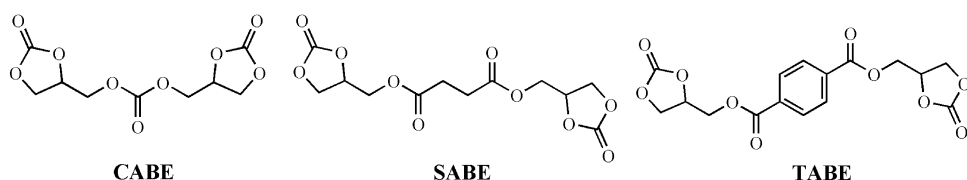
In spite of the successful introduction and increasing distribution of lithium-ion batteries in the world market, large-scale lithium-ion batteries with higher energy density are not yet commercially available for their practical application, such as electric vehicles, cellular phones, digital cameras and notebooks due to their associated safety problems [1–3]. With the scaling-up of lithium-ion batteries, the reduction of specific surface areas reduces the thermal dissipation rate. As heat accumulates in batteries, the thermal risk becomes much more serious than in normal batteries [4]. Therefore, in order to improve the safety performance of lithium-ion batteries, many researchers have investigated the flammability and thermal stability of the electrolyte at high temperature. The cyclic and linear carbonates are widely used for electrolytes of lithium-ion batteries. However, the linear carbonates have low flashing points and low boiling points, which is disadvantageous in terms of security [5]. By contrast, the cyclic carbonates have higher flashing points and boiling points, such as ethylene carbonate (EC), propylene carbonate (PC). Glycerol carbonate (GC) is a

rather new compound with many unique properties, such as high boiling point, high flash point, low flammability and low toxicity. Recently, it was reported that GC and its derivatives can be used as electrolytes in lithium-ion batteries instead of EC and PC [6,7]. Therefore, we designed and synthesized three new GC derivatives: carbonic acid bis-(2-oxo-[1,3]dioxolan-4-ylmethyl) ester (CABE), succinic acid bis-(2-oxo-[1,3]dioxolan-4-ylmethyl) ester (SABE) and terephthalic acid bis-(2-oxo-[1,3]dioxolan-4-ylmethyl) ester (TABE), which combined cyclic carbonate with various linear carbonate in order to have a better performance. Chemical structures of these compounds are shown in Fig. 1.

TG–FTIR technology is to transmit the escaping gas composition during the weight loss of sample in thermogravimeter to the infrared gas detection cell via constant temperature pipeline, through infrared detection, analysis and judgment the structure of escaping gas composition, proceeds quantitative and qualitative analysis, respectively. This method, which can conduct simultaneous and continuous real time analysis, is a useful technology for obtaining mass loss with time and evaluating the functional groups of the volatiles produced by pyrolysis [8–10]. This technique can give a deep insight into the evolution of pyrolysis and products information about the physical–chemical nature of the observed process. Therefore, it has been widely used in a variety of organic and inorganic materials in terms of thermal stability and thermal pyrolysis mechanism, even attracted more attention in the different research fields for different purposes [11–13].

\* Corresponding author at: College of Chemical Engineering and Material Science, Tianjin University of Science & Technology, No. 29, 13th Ave., TEDA, Tianjin 300457, China.

E-mail address: [jingliu@tust.edu.cn](mailto:jingliu@tust.edu.cn) (J. Liu).

**Fig. 1.** Chemical structure of compounds.

In present work, three new glycerol carbonate derivatives were synthesized, and their thermal pyrolysis behaviors were studied by the TG-FTIR technique. Furthermore, the theoretical calculations of the bond dissociation energy for these compounds were carried out for clarifying their thermal behaviors. Our work is focused on investigation of the relationship between molecular structure and thermal stability of three GC derivatives (CABE, OABE and TABE) with TG-FTIR analysis and theoretical calculation. This study may provide the useful information for molecular design and synthesis of new carbonates.

## 2. Experimental

### 2.1. Synthesis of compounds

#### 2.1.1. Synthesis of glycerol carbonate (GC)

In a 250 mL 3-necked round-bottomed glass flask equipped with a magnetic stirrer, a reflux condenser and a thermometer was placed 36.84 g (0.40 mol) of glycerol, 118 mL (1.40 mol) of dimethyl carbonate and 1.35 g (0.024 mol) of CaO as a catalyst. The mixture was stirred at 75 °C and kept subsequently under reflux for 5 h. After reaction, the solid catalyst (CaO) was removed by filtration. Then, the methanol and the residue of dimethyl carbonate were distilled off at 45 °C under reduced pressure to give colorless liquid glycerol carbonate (42.13 g, yield 89.19%) (reaction 1, **Scheme 1**).

<sup>1</sup>H NMR (400 MHz, Acetone-d<sub>6</sub>): δ 4.93–4.82(m, 1H), 4.58(t, J=8.4 Hz, 1H), 4.49–4.35(m, 2H), 3.89(d, J=12.5 Hz, 1H), 3.71(d, J=12.4 Hz, 1H). FTIR ( $\nu_{\max}$  cm<sup>-1</sup>): 3402, 2931, 1784, 1186, 1084.

#### 2.1.2. Synthesis of carbonic acid bis-(2-oxo-[1,3]dioxolan-4-ylmethyl) ester (CABE)

In a dry 250 mL 3-necked round-bottomed glass flask equipped with a magnetic stirrer, a funnel with pressure-equalising tube and a thermometer was placed 8.27 g (0.07 mol) of glycerol carbonate, 8.32 mL (0.06 mol) of triethylamine and 60 mL of anhydrous dichloromethane as solvent. A solution of bis(trichloromethyl) carbonate (2.97 g, 0.01 mol) in anhydrous dichloromethane (40 mL) was added dropwise to the above solution under nitrogen

atmosphere at 0 °C. The mixture was stirred at room temperature for 12 h. After reaction, the mixture was filtrated and the filtrate was evaporated under reduced pressure, the residues were purified by recrystallization from water to give the product (4.95 g, yield 63.05%) (reaction 2, **Scheme 1**).

<sup>1</sup>H NMR (400 MHz, DMSO-d<sub>6</sub>): δ 5.12–5.01 (m, 2H), 4.58–4.25(m, 8H) (Fig. S1(a)). FTIR ( $\nu_{\max}$  cm<sup>-1</sup>): 2925, 1793, 1761, 1176, 1052.

Supplementary Fig. S1 related to this article can be found, in the online version, at <http://dx.doi.org/10.1016/j.tca.2015.12.002>.

#### 2.1.3. Synthesis of succinic acid bis-(2-oxo-[1,3]dioxolan-4-ylmethyl) ester (SABE)

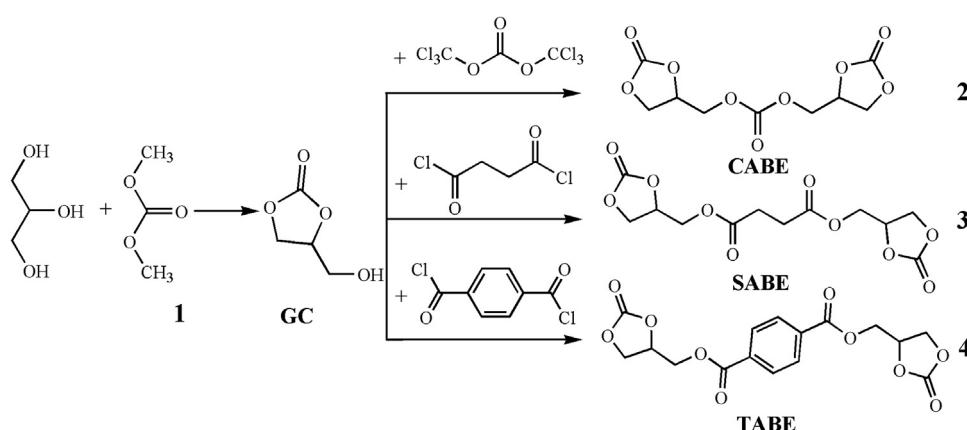
In a dry 100 mL 3-necked round-bottomed glass flask equipped with a magnetic stirrer, a funnel with pressure-equalising tube and a thermometer was placed 2.36 g (0.02 mol) of glycerol carbonate, 1.61 mL (0.02 mol) of pyridine and 30 mL of dry tetrahydrofuran as solvent. A solution of succinyl chloride (1.11 mL, 0.01 mol) in dry tetrahydrofuran (5 mL) was added dropwise to the above solution over 30 min under nitrogen atmosphere at –5 °C. The mixture was stirred for 4 h. After reaction, pyridine hydrochloride was removed by filtration. The filtrate was evaporated under reduced pressure, the residue was purified by recrystallization from acetone to give the product (1.00 g, yield 31.33%) (reaction 4, **Scheme 1**).

<sup>1</sup>H NMR (400 MHz, DMSO-d<sub>6</sub>): δ 5.08–4.99 (m, 2H), 4.57 (t, J=8.6 Hz, 2H), 4.35–4.21 (m, 6H), 2.63 (s, 4H) (Fig. S1(b)). FTIR ( $\nu_{\max}$  cm<sup>-1</sup>): 2929, 1785, 1736, 1164, 1054.

Supplementary Fig. S1 related to this article can be found, in the online version, at <http://dx.doi.org/10.1016/j.tca.2015.12.002>.

#### 2.1.4. Synthesis of terephthalic acid bis-(2-oxo-[1,3]dioxolan-4-ylmethyl) ester (TABE)

In a dry 100 mL 3-necked round-bottomed glass flask equipped with a magnetic stirrer, a funnel with pressure-equalising tube and a thermometer was placed 2.36 g (0.02 mol) of glycerol carbonate, 1.61 mL (0.02 mol) of pyridine and 30 mL dry tetrahydrofuran as solvent. A solution of terephthaloyl chloride (2.03 g, 0.01 mol) in dry tetrahydrofuran (15 mL) was added dropwise to the above

**Scheme 1.** The reaction route.

solution over 30 min under nitrogen atmosphere at 0 °C. The mixture was stirred for 4 h. After reaction, pyridine hydrochloride was removed by filtration. Then, the filtrate was evaporated under reduced pressure, and the residue was purified by recrystallization from dichloromethane to give the product (1.12 g, yield 30.61%) (reaction 2, Scheme 1).

<sup>1</sup>H NMR (400 MHz, CDCl<sub>3</sub>): δ 8.12 (s, 4H), 5.12–5.04 (m, 2H), 4.69–4.61 (m, 4H), 4.58–4.51 (m, 2H), 4.46–4.40 (m, 2H) (Fig. S1(c)). FTIR ( $\nu_{\text{max}}$  cm<sup>-1</sup>): 2923, 1786, 1723, 1275, 1052, 729.

Supplementary Fig. S1 related to this article can be found, in the online version, at <http://dx.doi.org/10.1016/j.tca.2015.12.002>.

## 2.2. TG-FTIR measurement

The TG-FTIR system was composed of a TA SDT-600 Instrument and a Bruker Tensor 27 FTIR spectrometer. For each TG-FTIR measurement, 10–20 mg sample was weighted into an open alumina crucible. The temperature was set from ambient temperature to 600 °C, the heating rate of the TG furnace was 20 °C min<sup>-1</sup>, and high purity (>99.999%) nitrogen gas with a flow rate of 140 mL min<sup>-1</sup> was used as carrier gas, this flow had to be kept high enough to avoid long residence time in the furnace and thus to prevent secondary reactions of the volatiles [14]. The transfer line used to connect TG and FTIR was a 1 m long stainless steel tube with an internal diameter of 2 mm, in order to reduce the possibility of gases condensing along the transfer line, the temperature in the gas cell and transfer line were set to 200 °C. The FTIR spectral region was set as 4000–600 cm<sup>-1</sup>, with the resolution of 4 cm<sup>-1</sup>, co-adding 16 scans per spectrum. The experiment started only when the whole system was stable. The experimental results of TG and FTIR were recorded automatically by a computer. Data was processed by the software OPUS 6.0 (Bruker Company, Germany).

## 2.3. Bond dissociation energy (BDE) calculation

The quantum chemistry calculations are performed using the Gaussian 09 program. The molecular structures are optimized at the M062X/cc-pVTZ level of theory and frequencies and energies of the molecules are calculated at the same level of theory. All molecular structures have no imaginary frequencies and are local minima on the potential energy surface. Formula (1), described by Blanksby and Ellison [15] is used to calculate the bond dissociation energy (BDE) for a dissociation process:  $R - Q \rightarrow R + Q$ .

$$D_0(R - Q) = E_0(R) + E_0(Q) - E_0(R - Q) \quad (1)$$

where  $D_0(R - Q)$ ,  $E_0(R)$ ,  $E_0(Q)$  and  $E_0(R - Q)$  denote to be calculated BDE, computed electronic energies at 0 K with zero-point energy (ZPE) corrections for  $R$ ,  $Q$  and  $R - Q$ , respectively.

## 3. Results and discussion

Fig. 2 presents the weight loss (TG), the corresponding derivative thermogram (DTG), Gram-Schmidt, the FTIR absorbance intensity of CO<sub>2</sub> and H<sub>2</sub>O curves of CABE, SABE and TABE as a function of temperature at a heating rate of 20 °C min<sup>-1</sup>. The TG curves showed the compounds weight loss during the thermal pyrolysis, and the Gram-Schmidt curves that based on vector analysis reconstructed the acquired interferograms, allowing the plots of the total evolved gases detected by the spectrometer to be obtained [16]. As can be seen in Fig. 2, the TG/DTG curves showed CABE had one weight loss stage, and SABE had two weight loss stages, while TABE had three weight loss stages. In other words, the major thermal pyrolysis reaction of CABE was finished in one step, SABE's major thermal pyrolysis reactions were finished in two steps, while the thermal pyrolysis processes of TABE were mainly divided into three steps.

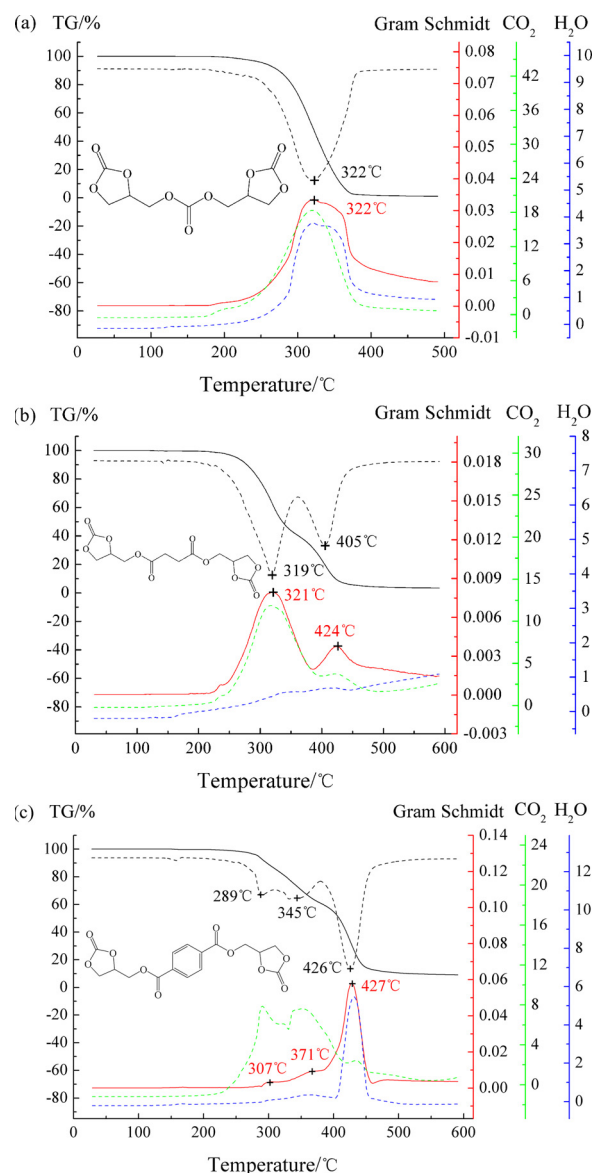


Fig. 2. The curves of TG, DTG, Gram-Schmidt, the FTIR absorbance intensity of CO<sub>2</sub> and H<sub>2</sub>O during the thermal pyrolysis of compounds: (a) CABE, (b) SABE and (c) TABE.

The weight loss of 99% of CABE took place in the temperature range of 210–385 °C. The first stage of SABE with weight loss of 60% happened in the temperature range of 210–361 °C, which was followed by the second weight losing stage in 361–500 °C, the overall weight loss of SABE was 97%. The first two slow weight losing stages of TABE took place in the temperature range of 230–309 °C and 309–380 °C, which was followed by a sharp weight loss of 52% in 380–500 °C, the overall weight loss of TABE measured at 600 °C was 91%. The Gram-Schmidt evolution peaks matched with the DTG peaks very well, and the temperature of the IR absorbance peaks coincided with that of the DTG peaks. There was a slight displacement between the peaks of the DTG and the Gram-Schmidt curves, because of the delay between the gas generation and its detection in the FTIR equipment [16].

We used 5% weight loss temperature as a measure to study the decomposition behavior [12]. The results of thermogravimetric analysis of three compounds were summarized in Table 1. According to the data in Table 1, we can see 5% weight loss temperature is high in the order of TABE > SABE > CABE, this result showed that

**Table 1**

Data of thermogravimetric analysis of CABE, SABE and TABE.

Compound	$t_{5\%}/^{\circ}\text{C}$	$t_{\max 1}/^{\circ}\text{C}$	$t_{\max 2}/^{\circ}\text{C}$	$t_{\max 3}/^{\circ}\text{C}$	Carbon residue rate/%
CABE	254	322	—	—	1
SABE	262	319	405	—	3
TABE	284	289	339	426	9

the thermal decomposition temperature of CABE, SABE and TABE gradually increased. In other words, their thermal stability was improved. This also means a benzene ring can make a better thermal stability for GC derivatives than a linear saturated hydrocarbon or carbonate block. According to the above mentioned, CABE, SABE and TABE behave differently during the thermal pyrolysis because of their different chemical structures.

In this work, TG-FTIR was used to explore the dynamic decomposition and analyze the gaseous products during the thermal pyrolysis of compounds. The 3D diagrams corresponding to gases evolved in the thermal pyrolysis of CABE, SABE and TABE were shown in Fig. 3. It showed the absorbance corresponding to the

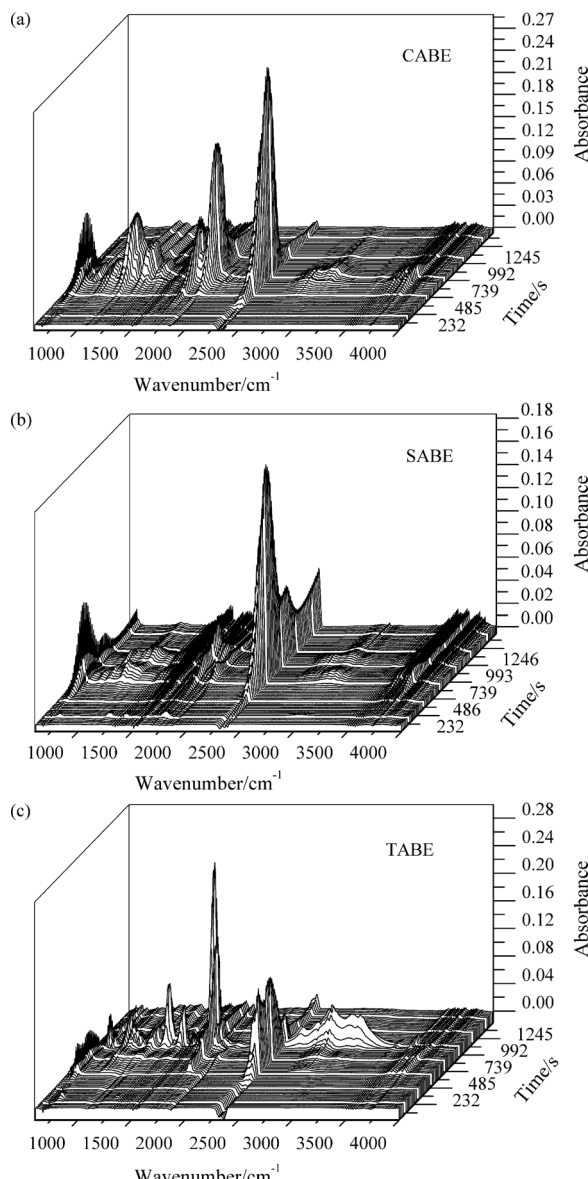


**Fig. 3.** The 3D diagrams corresponding to gases evolved in the thermal pyrolysis of compounds: (a) CABE, (b) SABE and (c) TABE.

vibrational modes of the different chemical bonds and functional groups versus the wavenumber and versus the time, and provides a clear qualitative picture of the overall information for the evolution of the FTIR spectra. Fig. 3 showed that the 3D diagrams of these three compounds were quite different from each other. It may mean that the thermal pyrolysis process of them should obey different pyrolysis pathway.

In order to study the volatile components released in the pyrolysis process, the FTIR spectra obtained at the maxima of the Gram-Schmidt curves (such as 322 °C of CABE, 321 °C and 424 °C of SABE, 307 °C, 371 °C and 427 °C of TABE) had been selected. The characteristic FTIR spectra of the gaseous products obtained at different temperatures were shown in Fig. 4. According to chemistry principles and some previous studies, some typical small molecular gaseous species can be easily identified by their

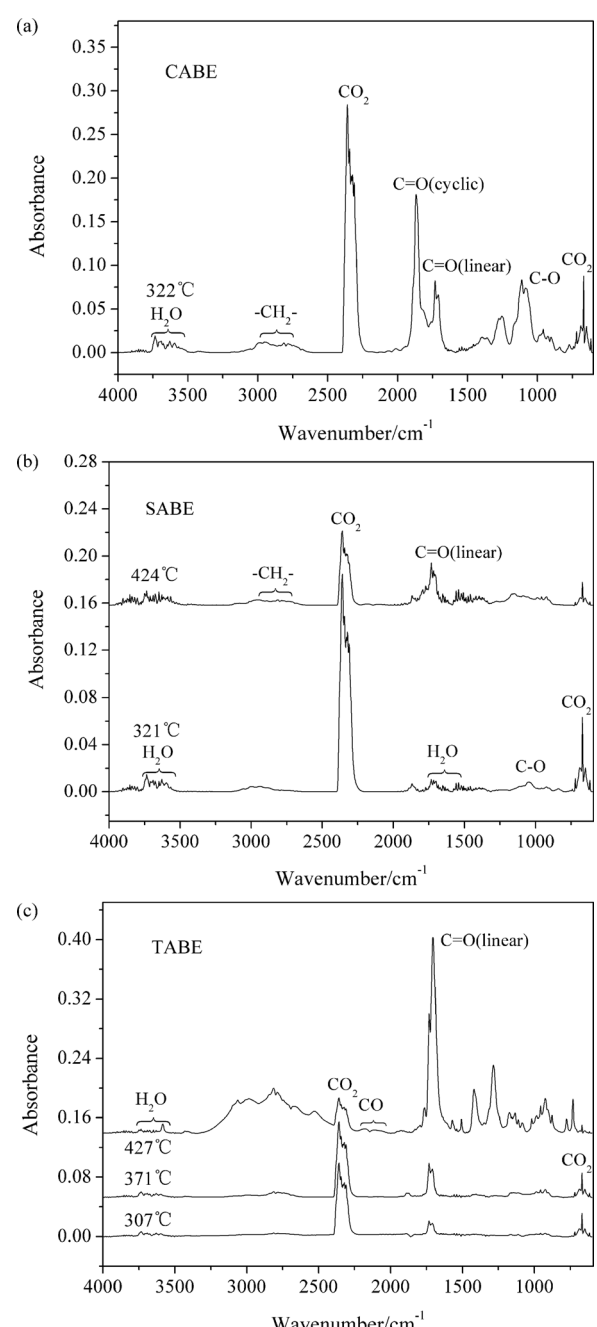


**Fig. 4.** The FTIR spectra of evolved gases from the thermal pyrolysis of compounds corresponding to the Gram-Schmidt peaks: (a) CABE, (b) SABE and (c) TABE.

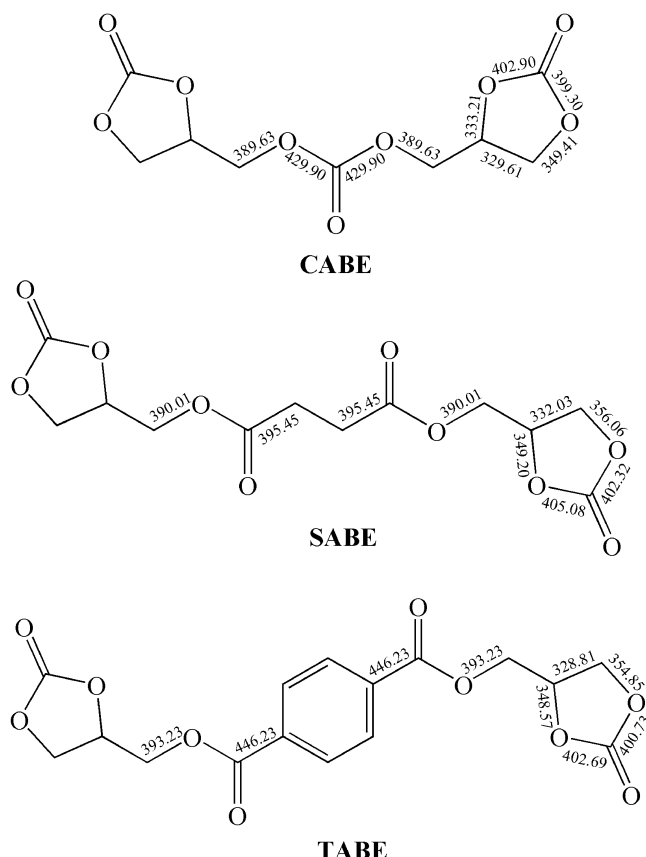


**Fig. 5.** The bond dissociation energy (BDE) of CABE, SABE and TABE (energy unit is kJ/mol).

characteristic absorbance:  $\text{CO}_2$  at  $2359\text{ cm}^{-1}$  and  $669\text{ cm}^{-1}$ ;  $\text{H}_2\text{O}$  at  $3400\text{--}4000\text{ cm}^{-1}$  and  $1300\text{--}1900\text{ cm}^{-1}$ ;  $\text{CO}$  at  $2175\text{ cm}^{-1}$  and  $2111\text{ cm}^{-1}$ . In order to further demonstrate the decomposition process of compounds, we calculated the bond dissociation energy (BDE) of CABE, SABE and TABE, and these data were shown in Fig. 5. BDE value can reflect the degree of difficulty of a bond fracture. The smaller the value is, the easier the bond cracks.

As Fig. 4(a) showed, when CABE was heated up to  $322^\circ\text{C}$ , there were several small molecular gaseous products released, such as  $\text{CO}_2$  and  $\text{H}_2\text{O}$ , which meant that some bond of compound cracked. For instance, the release of  $\text{CO}_2$  is mainly because of the cracking of ester group, which exhibits the most intense absorbance peak in the pyrolysis process. From the BDE data of CABE in Fig. 5, the BDE value of cyclic carbonate is very low, therefore the corresponding bonds ( $\text{C=C}$ ,  $\text{C-O}$ ) should fracture prior to others to generate  $\text{CO}_2$  and other substances. However, we found the  $\text{C=O}$  (cyclic) at  $1869\text{ cm}^{-1}$  in the FTIR spectra. This may be related to a low molecular weight of CABE. For the same type of ester, a low molecular weight always means a low boiling point. So, when the temperature reaches the boiling point of compound in the pyrolysis process, it will lead to part of the compound thermal cracking, there is also some compound escaping in the form of molecule at the same time. Carbon residue rate of CABE is very low, only 1%, which also partially supported above results.

Compared with CABE, the thermal pyrolysis process of SABE is more complicated. SABE has two major thermal pyrolysis steps. Once SABE was heated up to  $210^\circ\text{C}$ , the pyrolysis proceeded into the first pyrolysis stage. As can be seen in Fig. 4(b), there were plenty of  $\text{CO}_2$  and tiny amount of  $\text{H}_2\text{O}$  in the spectra of gaseous products at  $321^\circ\text{C}$ . Combining with the BDE data of SABE in Fig. 5, this indicates the main reaction is the  $\text{C-C}$ ,  $\text{C-O}$  bonds breakage of

cyclic carbonate in the first stage. After that, it stepped into the second pyrolysis stage. Compared with the former, CABE, we can see clearly the  $\text{C=O}$  (linear) at  $1732\text{ cm}^{-1}$  in the FTIR spectra at  $424^\circ\text{C}$ . It is mainly attributed to the BDE of linear  $\text{C-O}$  bond of compound is  $390.01\text{ kJ/mol}$ , higher than cyclic  $\text{C-C}$  bond ( $332.03\text{ kJ/mol}$ ). And linear ester group existed in the form of fragment.

For the molecular structure of SABE and TABE, the middle section of SABE's molecular structure is  $1,2\text{-ethylidene}$  ( $-\text{CH}_2\text{--CH}_2-$ ), while the middle section of TABE's molecular structure is  $1,4\text{-phenylene}$ . Different molecular structure leads to different pyrolysis process. The first two stages' weight loss of TABE was small, and their main gaseous product still was  $\text{CO}_2$ . This is also mainly because the  $\text{C-C}$ ,  $\text{C-O}$  bonds cracking of cyclic carbonate. When it went into the third pyrolysis stage, decomposition rate significantly increased. From the peak position of the FTIR spectra at  $427^\circ\text{C}$  in Fig. 4(c), we can infer the existence of  $\text{C=O}$  (linear) and phenylene, which suggests that BDE of linear  $\text{C-O}$  bond of compound is  $393.23\text{ kJ/mol}$ , higher than cyclic  $\text{C-C}$  bond ( $328.81\text{ kJ/mol}$ ). And linear ester group existed in the form of fragment.

#### 4. Conclusions

The thermal pyrolysis of CABE, SABE and TABE was investigated by TG-FTIR technology in the ambient temperature to  $600^\circ\text{C}$ . The results indicated that these three compounds had one, two, three weight loss stages, respectively. They had better thermal stability and their initial decomposition temperature was as high as  $200^\circ\text{C}$ , which can satisfy the using demand of the electrolyte in lithium-ion batteries. The thermogravimetric analysis showed that 5% weight loss temperature was increased in the following order: TABE > SABE > CABE, it means the thermal stability of TABE is better. And benzene ring was introduced to improve the thermal stability of the GC derivatives greater than saturated hydrocarbon block. And the TG-FTIR test also demonstrated the three GC derivatives behave quite differently during the thermal decomposition. According to the FTIR spectra at the maxima of the Gram-Schmidt curves and the theoretical calculation of bond dissociation energy (BDE), the  $\text{C-C}$ ,  $\text{C-O}$  bonds of cyclic carbonate fracture prior to others to generate  $\text{CO}_2$  and other products. For CABE, part of the compound escaped in the form of molecule in the pyrolysis process because of its' low boiling point. For SABE and TABE, they continued to crack, the  $\text{C-O}$  bond nearby cyclic carbonate fracture to produce linear ester in the form of fragment.

#### Acknowledgements

This work was financially supported by the National Natural Science Foundation of China (Grant No. 21373150). The authors would like to thank software application engineer Xuju Jiang at Bruker Company for her help on TG-FTIR measurement and the use of the software OPUS 6.0.

#### References

- [1] E.-G. Shim, T.-H. Nam, J.-G. Kim, H.-S. Kim, S.-I. Moon, Effects of functional electrolyte additives for Li-ion batteries, *J. Power Sources* 172 (2007) 901–907.
- [2] E.-G. Shim, T.-H. Nam, J.-G. Kim, H.-S. Kim, S.-I. Moon, Effect of vinyl acetate plus vinylene carbonate and vinyl ethylene carbonate plus biphenyl as electrolyte additives on the electrochemical performance of Li-ion batteries, *Electrochim. Acta* 53 (2007) 650–656.
- [3] D. Aurbach, K. Gamolsky, B. Markovsky, Y. Gofer, M. Schmidt, U. Heider, On the use of vinylene carbonate (VC) as an additive to electrolyte solutions for Li-ion batteries, *Electrochim. Acta* 47 (2002) 1423–1439.
- [4] L. Zhao, S. Okada, J.-I. Yamaki, Effect of VC additive on MFA-based electrolyte in Li-ion batteries, *J. Power Sources* 244 (2013) 369–374.
- [5] S.-C. Kinoshita, M. Kotato, Y. Sakata, M. Ue, Y. Watanabe, H. Morimoto, S.-I. Tobishima, Effects of cyclic carbonates as additives to  $\gamma$ -butyrolactone electrolytes for rechargeable lithium cells, *J. Power Sources* 183 (2008) 755–760.

- [6] W.K. Teng, G.C. Ngoh, R. Yusoff, M.K. Aroua, A review on the performance of glycerol carbonate production via catalytic transesterification: effects of influencing parameters, *Energy Convers. Manag.* 88 (2014) 484–497.
- [7] G.V. Waghamare, M.D. Vetal, V.K. Rathod, Ultrasound assisted enzyme catalyzed synthesis of glycerol carbonate from glycerol and dimethyl carbonate, *Ulras. Sonochem.* 22 (2015) 311–316.
- [8] D. Chen, D. Liu, H. Zhang, Y. Chen, Q. Li, Bamboo pyrolysis using TG–FTIR and a lab-scale reactor: analysis of pyrolysis behavior, product properties, and carbon and energy yields, *Fuel* 148 (2015) 79–86.
- [9] S. Jingyan, L. Yuwen, W. Zhiyong, W. Cunxin, Investigation of thermal decomposition of ascorbic acid by TG–FTIR and thermal kinetics analysis, *J. Pharm. Biomed. Anal.* 77 (2013) 116–119.
- [10] J. Li, Z. Wang, X. Yang, L. Hu, Y. Liu, C. Wang, Evaluate the pyrolysis pathway of glycine and glycylglycine by TG–FTIR, *J. Anal. Appl. Pyrolysis* 80 (2007) 247–253.
- [11] T. Xu, X. Huang, Study on combustion mechanism of asphalt binder by using TG–FTIR technique, *Fuel* 89 (2010) 2185–2190.
- [12] X.H. Li, Y.Z. Meng, Q. Zhu, S.C. Tjong, Thermal decomposition characteristics of poly(propylene carbonate) using TG/IR and Py-GC/MS techniques, *Polym. Degrad. Stabil.* 81 (2003) 157–165.
- [13] A. Meng, H. Zhou, L. Qin, Y. Zhang, Q. Li, Quantitative and kinetic TG–FTIR investigation on three kinds of biomass pyrolysis, *J. Anal. Appl. Pyrolysis* 104 (2013) 28–37.
- [14] J. Giuntoli, W. de Jong, S. Arvelakis, H. Spliehoff, A.H.M. Verkooijen, Quantitative and kinetic TG–FTIR study of biomass residue pyrolysis: dry distiller's grains with solubles (DDGS) and chicken manure, *J. Anal. Appl. Pyrolysis* 85 (2009) 301–312.
- [15] S.J. Blanksby, G.B. Ellison, Bond dissociation energies of organic molecules, *Acc. Chem. Res.* 36 (2003) 255–263.
- [16] A. Marcilla, A. Gómez, S. Menargues, TG/FTIR study of the thermal pyrolysis of EVA copolymers, *J. Anal. Appl. Pyrol.* 74 (2005) 224–230.